Proceedings of 10th International Conference on Precision, Meso, Micro and Nano Engineering (COPEN 10)
December 07 – 09, 2017, Indian Institute of Technology Madras, Chennai – 600 036 INDIA

Effect of welding speed on weld-bead quality aspects in bead-on-plate laser welding of NiTinol by Yb-fiber laser

Susmita Datta*, Mohammad Shahid Raza, Partha Saha and Dilip Kumar Pratihar

Department of Mechanical Engineering,
Indian Institute of Technology Kharagpur, Kharagpur - 721302, INDIA

Abstract

Laser welding is a promising method for joining of NiTinol, which has some superior properties like shape memory effect, super elasticity, corrosion resistance, and good biocompatibility. This experimental work evaluates different aspects of weld bead quality and corrosion properties of bead-on-plate Yb-fiber laser welded samples of NiTinol. Laser was operated in continuous wave mode and welding was carried out on 2mm thick sheet by varying welding speed for constant power. Bead geometry quality aspects show a decreasing trend for increasing scan speed for a constant power. Near the fusion line, the solidification process is followed by planar and cellular growth. When solidification front moves toward the weld centre-line, the dendritic growth occurs. Presence of brittle intermetallics (Ni_3Ti, Ti_2Ni) was identified by phase analysis with the help of XRD analysis. Microhardness values gradually increased from 220 $HVN_{0.05}$ at weld centre line to 350 $HVN_{0.05}$ at base metal, depending upon the grain structure. Polarization resistance for the base metal was found to be 443.6 Ohm/cm^2, but the value was increased many times for welded samples. Due to better corrosion resistance property of the welded zone, laser welding can be used as an efficient joining technology for biomedical devices made of NiTinol.

Keywords: Laser welding, NiTinol, Bead geometry quality aspects, Microhardness, Intermetallics, Corrosion resistance

1. INTRODUCTION

As NiTinol is having unique properties like shape memory effect, pseudoelasticity and biocompatibility, it is considered one of the popular and new smart materials used in different fields, such as aviation and aerospace applications, hydrospace applications, MEMS applications, structural and civil applications, and medical applications [1-12]. Poor machinibility and lack of joining techniques of NiTinol to itself and to other materials are root of all challenges for manufacturing components with this material.

Precision, good control of heat input, high processing speed, good weld bead profile, narrow heat affected zone width, minimum residual stress and distortion are the superior qualities of laser welding process, which make it an interesting joining technique for materials with limited weldability [13-14]. Formation of Ti_2Ni and Ni_3Ti brittle intermetallic phases in weld metal is the main problem associated with welding of NiTinol [15–16]. During cooling, segregation of titanium helps in the formation of Ti_2Ni precipitates at grain boundaries. Precipitations of brittle intermetallic phases may greatly affect mechanical properties of the alloy, as they act as crack initiation sites [17]. Higher solidification rate reduces the amount of deposited intermetallic phases in weld metal [18]. As higher solidification rate is achieved in laser welding [19], these methods are very useful for welding of materials which are sensitive to the formation of brittle phases due to welding. CO_2 gas laser [16, 20], Nd:YAG solid state laser [21–24] and fiber laser [25-26]were used for welding NiTinol shape memory alloy.

In this study the effect of scan speed on bead geometry profile, bead geometry quality aspects, variation of microstructure at different zones of welded sample, phase analysis of welded as well as parent material, variation of microhardness value across weld-bead, and corrosion behaviour of welded and parent samples were studied for bead-on-plate welding of NiTinol, using fiber laser system. Variation of laser weld-bead profile of NiTinol with variation of scan speed at a constant power for 2 mm thick sheet was not reported in existing literature.

2. MATERIAL AND METHODS

The work piece was 2 mm thick sheet of NiTinol (52 atomic % Ni, 48 atomic % Ti) of dimension 25 mm × 60 mm. A 2 kW Yb-fiber laser system having a focal length of 200mm and focal spot diameter varying from 250 µm to 400 µm was used to make the bead-on-plate laser weld. These samples were acid cleaned in an acid mixture of HF: HNO_3:H_2O=1:5:10 for 20 S to remove any kind of oxide layer prior to welding. Argon gas shielding at a flow rate of 7lpm was used as to protect the weld pool from atmospheric contamination. The focal point of the laser was kept on the top surface of the sample to get the maximum power density there. Welding was done at 1700 W by varying scan speed from 2000 mm/min to 5000 mm/min. After welding the beads were cut in the middle of the track to get the cross-section of the best portion of the weld-bead. The cut edges were polished mechanically by SiC paper varying from grit size of 600 to2400 and then polished with a diamond paste of 1 µm along the cross-section of each weld track. This was followed by etching the polished cross-section with the acid mixture of HF: HNO_3:H_2O= 3:7:21 for 10 s to reveal the weld bead profile. Zeiss zoom microscope was used to obtain the weld bead geometry data. For preparing metallographic samples specimens were cold mounted by epoxy and then mechanically polished in a similar way. Scanning electron microscope (SEM) [Model: EVO 18 Research, Make: Zeiss] was used to reveal the microstructure. XRD analyses on welded as well as un-welded samples were done to get the idea about the formation of new phases during

*Author to whom correspondence should be made, Email: susmita.prod @gmail.com

ISBN: 978-93-80689-28-9

welding using Cu-Kα radiation. To get the idea of variation of microhardness along the base metal, HAZ and weld-bead, Vicker's microhardness test was performed across the weld zone, heat affected zone (HAZ) and the base metal for the weld-bead of 1700 W power and scan speed of 5000 mm/min with a microhardness tester [Model: S.Auto, Make: Omnitech]. A 50 g load and a dwell time of 10 s were used. The cross-section of the bead was polished and etched before microhardness test. Corrosion behavior of the both welded samples as well as the parent material was determined by potentiodynamic polarization test in simulated body fluid (SBF) at 37.5ºC. Corrosion test was carried out based on the standard ASTM G61-86 using Biologic SP150 electrochemical work station having Ag-AgCl as the reference electrode, Platinum as a counter electrode and sample as working electrode. After an initial delay of 3600 s to obtain the stability of open circuit potential, Tafel plot experiment was conducted from −1 V/SCE to + 1 V/SCE at the scan rate 0.8 mV/s. Biologic soft electrochemistry software was employed to get the values of corrosion current density (I_{corr}), polarization resistance (R_p) and corrosion potential (E_{corr}). For each and every result 3 replicates were considered and error bars for Fig. 2 and Fig. 6(b) were inserted.

3. RESULTS AND DISCUSSION

3.1 Weld-bead Geometry

Bead geometry changed from bowl shaped top with a small leg to glass shape through wine glass shape with decreasing scan speed. For the line-energy value (power/velocity) 20 J/mm partial penetrations welding occurred but above 51 J/mm line energy, burning of metal took place. Full penetrated narrow bead was obtained for line energy range 25 J/mm to 35 J/mm. Near Gaussian beam intensity distribution and conduction mode of welding was the cause behind this kind of bead geometry formation. The variation of bead width and heat affected zone width at the top surface is plotted for varying scan speed. Both indicated the decreasing trend with increasing scan speed. The standard deviations for bead width were varied from 2.2% to 4.2% but those for HAZ width were 1.3% to 4.7%.

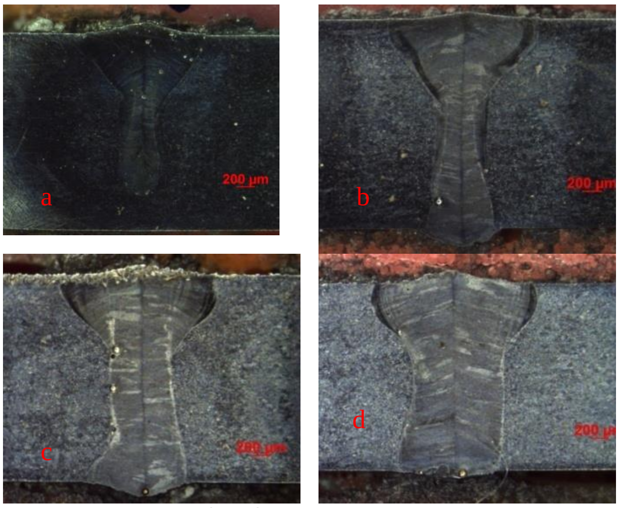

Fig. 1 Weld-bead profiles for (a) v=5000 mm/min, (b) v=4000 mm/min, (c) v=3000 mm/min, and (d) v=2000mm/min

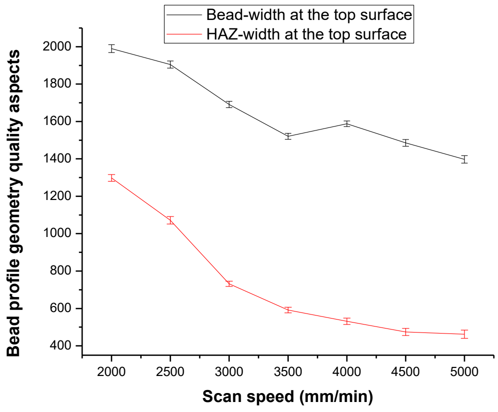

Fig. 2 Variations of bead-width and HAZ-width of weld-bead

3.2 Microstructure

Temperature gradient (G), solidification rate (R), under cooling (ΔT) and alloy composition controls the microstructure of weld bead. From the fusion boundary to the weld centre-line, the solidification rate increased but the temperature gradient gradually decreased. Therefore, the ratio of G/R at the fusion boundary was highest. The microstructure near the fusion boundary of the weld showed presence of epitaxial growth. The grain growth initiated from the HAZ at the fusion boundary and proceeded toward the weld center-line. Near the fusion boundary, a region of small columnar grains formed. The fusion zone consisted of larger columnar dendrite grains oriented normal to the centerline. When solidification front moved toward the weld centre-line, dendrite growth occurred in the centre of the weld.

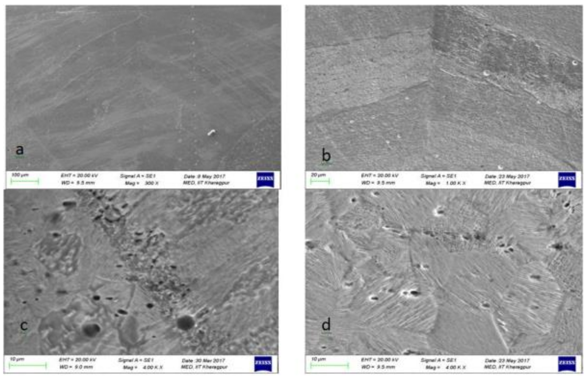

Fig. 3 Microstructure of the welded sample (a) Weld-bead, (b) Weld-bead center-line, (c) Interface of weld bead and HAZ, (d) parent material.

3.3 Microhardness

The base metal showed the highest value of microhardness (around 350 $HVN_{0.05}$) due to the finest grain structure and more chemical and microstructural homogeneity than the weld zone. Though there was some instability on the measured values, a clear trend of continuously increasing hardness value, from the weld zone towards the base metal, was observed. The cause of this kind of variations of microhardness was that the area near the fusion zone experienced relatively slow cooling rate, and hence had a coarse grain structure, while the area near the base metal had fine grained microstructure due to high cooling rate and steeper thermal gradients. The minimum value of microhardness in weld centre-line was around 220 $HVN_{0.05}$.

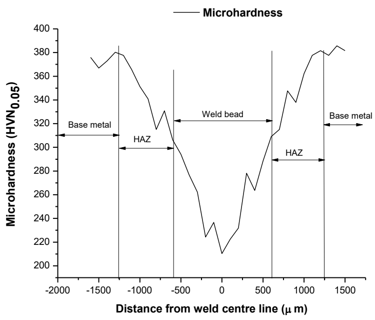

Fig. 4 Variation of microhardness across bead for v=5000 mm/min

3.4 XRD Analysis

From the XRD pattern of the parent material, it was clear that both austenite and martensite phases were present in the parent material at room temperature. In the welded zone, presence of different intermetallics, such as Ni_3Ti, Ti_2Ni was observed. According to phase diagram, the Ni_3Ti could be formed in the Ni rich side, as a result of the reaction NiTi + liquid⇒ Ni_3Ti, and Ti_2Ni could be formed in Ti rich side by the reaction of NiTi + liquid⇒ Ti_2Ni.These brittle intermetallics got accumulated on grain boundaries of weld metal. As a result of this the tensile strength of the welded sample would reduce by the welding.

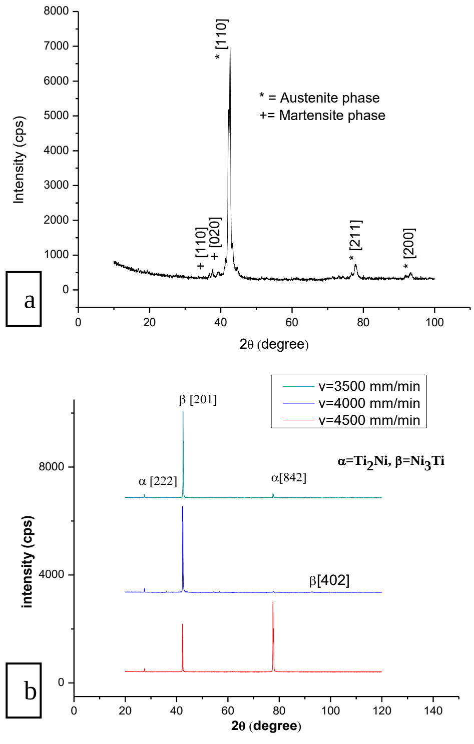

Fig. 5 Phase analysis of (a) parent material (b) welded samples at different scan speeds.

3.5 Corrosion Test

From Fig. 6, it is prominent that $R_p$values of welded samples were higher than those of the parent material, which indicated that they have better corrosion resistance compared to the parent material. Corrosion resistance of NiTinol alloy is dependent on the stability of passive film of TiO_2 on the surface of the material. This passive film acts a barrier against release of Ni ions from NiTinol by changing the oxidation pathways of Ni. From R_p values of parent and welded sample it was clear that the stability of passive TiO_2 layer was increased by welding, and hence the welded samples possessed good corrosion resistance property. Standard deviation for R_P values varied from 4% to 6%.

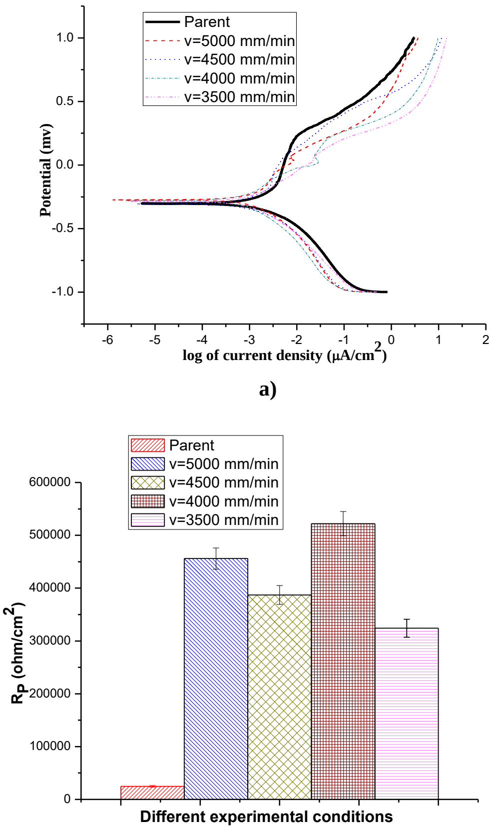

b)

Fig. 6 (a) Potentiodynamic polarization curves for the parent and welded samples obtained for different experimental runs, (b) Polarization resistance for parent and welded samples.

4. CONCLUSIONS

a) From this study on laser welding of NiTinol sheets, it was clear that good quality welds in terms of weld bead geometry would be produced for a line energy range of 25-35 J/mm. Above the line energy value of 51 J/mm, materials would get burnt instead of getting welded for the sheet thickness of 2 mm. Welding with a partial penetration occurred below the line energy value of 20 J/mm. The quality aspects of weld bead-geometry, like HAZ width and weld-bead width were reduced with increasing scan speed for a constant power value, as the line energy decreased.
b) Microhardness increased from weld centre-line to base metal through HAZ depending upon grain growth during solidification.
c) From phase analysis of the material, it was clear that some brittle intermetallics, which might have effect on weld strength, were formed during welding.
d) From the corrosion test, it was clear that the welded samples were more corrosion resistant than the parent material.

References

[1] Otsuka, K., and C. M. Wayman. "Mechanism of shape memory effect and superelasticity." Shape memory materials: 27-48, 1998.

[2] Predki, Wolfgang, Adam Knopik, and Björn Bauer. "Engineering applications of NiTi shape memory alloys." Materials Science and Engineering: A 481: 598-60, 2008.

[3] Duerig, T. W., A. Pelton, and D. Stöckel. "An overview of nitinol medical applications." Materials Science and Engineering: A 273: 149-160, 1999.

[4] Kannan, T. Deepan Bharathi, T. Ramesh, and P. Sathiya. "A Review of Similar and Dissimilar Micro-joining of Nitinol." JOM 68.4: 1227-1245, 2016.

[5] Morgan, N. B. "Medical shape memory alloy applications—the market and its products." Materials Science and Engineering: A 378.1: 16-23, 2004.

[6] Duerig, T. W., A. Pelton, and D. Stöckel. "An overview of nitinol medical applications." Materials Science and Engineering: A 273: 149-160, 1999.

[7] Song, Gangbing, N. Ma, and H-N. Li. "Applications of shape memory alloys in civil structures." Engineering structures 28.9: 1266-1274, 2006.

[8] Saadat, S., et al. "An overview of vibration and seismic applications of NiTi shape memory alloy." Smart materials and structures 11.2: 218, 2002.

[9] Dolce, Mauro, and Donatello Cardone. "Mechanical behaviour of shape memory alloys for seismic applications 2. Austenite NiTi wires subjected to tension." International Journal of Mechanical Sciences 43.11: 2657-2677, 2001.

[10] Dolce, Mauro, and Donatello Cardone. "Mechanical behaviour of shape memory alloys for seismic applications 1. Martensite and austenite NiTi bars subjected to torsion." International Journal of Mechanical Sciences 43.11 (2001): 2631-2656, 2004.

[11] Hartl, Darren J., and Dimitris C. Lagoudas. "Aerospace applications of shape memory alloys." Proceedings of the Institution of Mechanical Engineers, Part G: Journal of Aerospace Engineering 221.4: 535-552, 2007.

[12] Kahn, H., M. A. Huff, and A. H. Heuer. "The TiNi shape-memory alloy and its applications for MEMS." Journal of Micromechanics and Micro-engineering8.3: 213, 1998

[13] Quintino, L., et al. "Fracture analysis of Ag nanobrazing of NiTi to Ti alloy." Soldagem & Inspeção 18.3: 281-286, 2013.

[14] Çam, G., and M. Koçak. "Joining of Advanced Materials." Encyclopedia of Life Support Systems, Area 6: Materials science and engineering, Topic 6.36. 4: Material processing and manufacturing technologie (1998).

[15] Sun, Z., and J. C. Ion. "Laser welding of dissimilar metal combinations." Journal of Materials Science 30.17: 4205-4214, 1995.

[16] Yan, X. J., D. Z. Yang, and X. P. Liu. "Corrosion behavior of a laser-welded NiTi shape memory alloy." Materials Characterization 58.7: 623-628,2007.

[17] Hsu, Y. T., et al. "Effect of CO2 laser welding on the shape-memory and corrosion characteristics of TiNi alloys." Metallurgical and materials transactions A 32.3: 569-576, 2001.

[18] Lopez, H. F., A. Salinas-Rodriguez, and J. L. Rodriguez-Galicia. "Microstructural aspects of precipitation and martensitic transformation in a Ti-rich Ni-Ti alloy." Scripta materialia 34.4: 659-664, 1996.

[19] Borrisutthekul, Rattana, et al. "Suppression of intermetallic reaction layer formation by controlling heat flow in dissimilar joining of steel and aluminum alloy." Materials Science and Engineering: A 467.1: 108-113, 2007.

[20] Allmen, Martin V., and Andreas Blatter. Laser-beam interactions with materials: physical principles and applications. Vol. 2. Springer Science & Business Media, 2013.

[21] Tuissi, A., et al. "CO2 laser welding of NiTi/Ni-based alloys." Proc. Int. Conf. Shape Mem. Superelastic Technol. 2004.

[22] Maletta, C., et al. "Fracture behaviour of nickel-titanium laser welded joints." Journal of materials engineering and performance 18.5-6: 569-574, 2009.

[23] Song, Y. G., et al. "The influence of laser welding parameters on the microstructure and mechanical property of the as-jointed NiTi alloy wires." Materials letters 62.15: 2325-2328, 2008.

[24] Gugel, H., A. Schuermann, and W. Theisen. "Laser welding of NiTi wires." Materials Science and Engineering: A 481: 668-671, 2008.

[25] Chan, Chi Wai, and H. C. Man. "Laser welding of thin foil nickel–titanium shape memory alloy." Optics and Lasers in Engineering 49.1: 121-126, 2011.

[26] Miranda, R. M., et al. "Fiber laser welding of NiTi to Ti-6Al-4V." The International Journal of Advanced Manufacturing Technology 81.9-12: 1533-1538, 2015.